

# An insight into the protonation property of a diiron azadithiolate complex pertinent to the active site of Fe-only hydrogenases†

Weibing Dong,<sup>a</sup> Mei Wang,<sup>\*a</sup> Xiaoyang Liu,<sup>ab</sup> Kun Jin,<sup>a</sup> Guanghua Li,<sup>b</sup> Fujun Wang<sup>a</sup> and Licheng Sun<sup>\*ac</sup>

Received (in Cambridge, UK) 19th September 2005, Accepted 31st October 2005

First published as an Advance Article on the web 22nd November 2005

DOI: 10.1039/b513270c

Protonation of  $[(\mu\text{-SCH}_2)_2\text{N}(\text{C}_6\text{H}_4\text{-}p\text{-NO}_2)]\{\text{Fe}(\text{CO})_2(\text{PMe}_3)_2\}_2$  in the presence of 4 equiv. of HOTf afforded two species, a  $\mu$ -hydride diiron complex, the molecular structure of which was crystallographically characterized, and a  $\mu$ -S-protonated species, which was readily deprotonated in the presence of pyridine.

In recent years, special attention has been paid to the molecular models of the Fe-only hydrogenase active site due to its remarkable efficiency in  $\text{H}_2$  production and its structural resemblance to well-known complexes  $[(\mu\text{-SR})_2\{\text{Fe}(\text{CO})_2\text{L}\}_2]$ .<sup>1</sup> One of the challenging issues is to elucidate the mechanism of enzymatic hydrogen production and uptake by figuring out which heteroatom of the diiron substrate might act as a favorable internal basic site in the heterolytic cleavage of  $\text{H}_2$ , or as a preferred acidic site in a protonated form in the enzymatic  $\text{H}_2$ -evolution. The DFT calculations relevant to the Fe-only hydrogenase active site and its molecular models suggested three controversial pathways for the  $\text{H}_2$ -heterolytic splitting with the formation of the iron hydride species, that is, protonation on the N atom, either in the  $\text{CN}^-$  ligand or in the 2-azapropane bridge,<sup>2</sup> or protonation on one of the  $\mu$ -S atoms.<sup>3</sup> The experimental proof for the formation of the  $\mu$ -S protonated species of the 2Fe2S model complexes is as yet undisclosed.

Although the protonation of model complexes bearing a pdt-bridge (pdt = 1,3-propanedithiolato) and their catalytic properties for electrochemical proton reduction are well studied,<sup>4–10</sup> the diiron azadithiolate model complexes and their reactivity towards proton acids have been less described so far. The rare reports on the protonation properties and electrochemical proton reduction of the adt-bridged (adt = 2-azapropanedithiolato) diiron complexes are confined to the all-carbonyl complexes.<sup>11</sup> To have an insight into the protophilic property of the  $\text{PMe}_3$ -disubstituted diiron azadithiolate complex,  $[(\mu\text{-SCH}_2)_2\text{N}(\text{C}_6\text{H}_4\text{-}p\text{-NO}_2)]\{\text{Fe}(\text{CO})_2(\text{PMe}_3)_2\}_2$  (**2**) was prepared and the protonation process of **2** was explored by IR,  $^{31}\text{P}\{^1\text{H}\}$  and  $^1\text{H}$  NMR spectroscopy in the presence of different amounts of HOTf. Here we describe the spectroscopic evidence for the protonation

property of **2** on the iron and the  $\mu$ -S atoms, and the molecular structures of **2** and its  $\mu$ -hydride species  $[\text{Z}(\text{FeHF}_e)]^+[\text{PF}_6]^-$ .

The all-carbonyl diiron azadithiolate complex  $[(\mu\text{-SCH}_2)_2\text{N}(\text{C}_6\text{H}_4\text{-}p\text{-NO}_2)]\text{Fe}_2(\text{CO})_6$  (**1**) was prepared according to the procedure of Rauchfuss *et al.*<sup>12</sup> The  $\text{PMe}_3$ -disubstituted complex **2** was obtained in a good yield by double CO-displacement of **1** with 4 equiv. of  $\text{PMe}_3$  in toluene. The  $\nu(\text{CO})$  values of **2** at 1985, 1949 and  $1906\text{ cm}^{-1}$  (Fig. 1, left (a)) were substantially lowered as compared with those of **1** at 2078, 2040 and  $2001\text{ cm}^{-1}$ .<sup>11c</sup> The selected region ( $\delta = 2.5\text{--}9.0$ ) of the  $^1\text{H}$  NMR spectrum of **2** is shown in Fig. 2 (a).

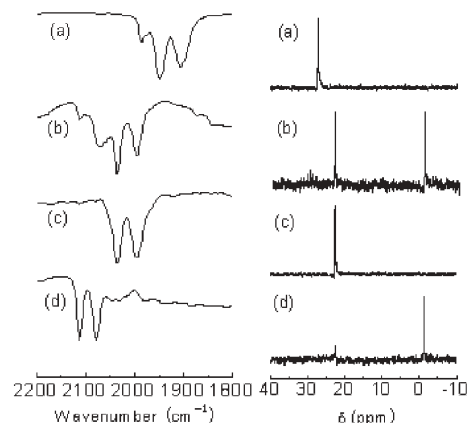


Fig. 1 FT-IR (left) and  $^{31}\text{P}\{^1\text{H}\}$  NMR (right) spectra of (a) **2** in  $\text{CH}_3\text{CN}$ , (b) + 4 equiv. HOTf, (c)  $[\text{Z}(\text{FeHF}_e)]^+[\text{PF}_6]^-$  in  $\text{CH}_3\text{CN}$ , (d)  $[\text{Z}(\text{SH})]^+[\text{OTf}]^-$  in  $\text{CH}_3\text{CN}$ , containing a small amount of  $[\text{Z}(\text{FeHF}_e)]^+[\text{OTf}]^-$ .

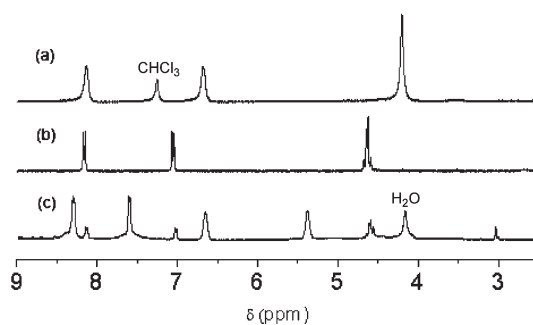


Fig. 2  $^1\text{H}$  NMR spectra of the selected region: (a) **2** in  $\text{CDCl}_3$ , (b)  $[\text{Z}(\text{FeHF}_e)]^+[\text{PF}_6]^-$  in  $\text{CD}_3\text{CN}$ , (c)  $[\text{Z}(\text{SH})]^+[\text{OTf}]^-$  in  $\text{CD}_3\text{CN}$ , containing a small amount of  $[\text{Z}(\text{FeHF}_e)]^+[\text{OTf}]^-$ .

<sup>a</sup>State Key Laboratory of Fine Chemicals, Dalian University of Technology, Zhongshan Road 158-46, 116012 Dalian, P. R. China. E-mail: symbuono@dut.edu.cn; Fax: +86 411 83702185; Tel: +86 411 88993886

<sup>b</sup>State Key Laboratory of Inorganic Synthesis and Preparative Chemistry, Jilin University, 130012 Changchun, P. R. China

<sup>c</sup>KTH Chemistry, Organic Chemistry, Royal Institute of Technology, 10044 Stockholm, Sweden

† Electronic supplementary information (ESI) available: Experimental details and selected bond lengths and angles of **2** and  $[\text{Z}(\text{FeHF}_e)]^+$ . See DOI: 10.1039/b513270c

To get a preliminary perception of the protonation process of **2**, the *in situ* IR and  $^{31}\text{P}\{^1\text{H}\}$  NMR spectra of **2** in different amounts of HOTf were recorded in  $\text{CH}_3\text{CN}$ . The three  $\nu(\text{CO})$  bands in the IR and the signal in the  $^{31}\text{P}\{^1\text{H}\}$  NMR spectra of **2** (Fig. 1 (a)) did not display any noticeable shift as an equiv. of HOTf was added to the  $\text{CH}_3\text{CN}$  solution of **2**. With an increase of the molar ratio of HOTf up to 1 : 4 (**2** : HOTf, mol/mol), the  $\nu(\text{CO})$  bands of **2** completely disappeared and four blue-shifted bands at 2111, 2071, 2035 and 1995  $\text{cm}^{-1}$  were observed (Fig. 1, left (b)). At the same time two new signals at  $\delta = 22.52$  and  $-1.09$  appeared in the  $^{31}\text{P}\{^1\text{H}\}$  NMR spectrum (Fig. 1, right (b)), shifting high field by 4.67 and 28.28 ppm, respectively, as compared with that of the non-protonated complex **2**. It is noteworthy that the signal at  $\delta = -1.09$  vanished when an excess of pyridine was added, accompanied by regeneration of the signal of **2** at  $\delta = 27.19$ , while the intensity of the signal at  $\delta = 22.52$  did not show observable change. The IR and  $^{31}\text{P}\{^1\text{H}\}$  NMR spectra imply that two different protonated species of **2** are formed in a 1 : 4 molar ratio of **2** : HOTf in  $\text{CH}_3\text{CN}$ . The one with the  $^{31}\text{P}$  NMR signal at  $\delta = 22.52$  is relatively stable in the presence of excess pyridine, and the other protonated species with the signal at  $\delta = -1.09$  is readily deprotonated by pyridine.

The pure  $\mu$ -hydride diiron complex  $[\mathbf{2}(\text{FeHFe})]^+$  was isolated as a  $\text{PF}_6^-$  salt by addition of a few drops of saturated aqueous  $\text{NH}_4\text{PF}_6$  solution to the  $\text{CH}_2\text{Cl}_2$ -EtOH (2 : 15, v/v) solution of **2** and HCl (48 equiv., 12 M). Complex  $[\mathbf{2}(\text{FeHFe})]^+[\text{PF}_6]^-$  is quite stable in the solid state and in  $\text{O}_2$ -free neutral solution. The  $\nu(\text{CO})$  frequencies of  $[\mathbf{2}(\text{FeHFe})]^+$  at 2035 and 1995  $\text{cm}^{-1}$  (Fig. 1, left (c)) and the signal of the  $\text{PMe}_3$  ligands at  $\delta = 22.52$  (Fig. 1, right (c)) indicate that  $[\mathbf{2}(\text{FeHFe})]^+$  is one of the two protonated species detected in the  $\text{CH}_3\text{CN}$  solution of **2** and HOTf. The high-field triplet at  $\delta = -15.02$  with  $J_{\text{PH}} = 21.7$  Hz in the  $^1\text{H}$  NMR spectrum provides an unambiguous proof for the formation of the  $\mu$ -hydride diiron complex  $[\mathbf{2}(\text{FeHFe})]^+$ . The  $^1\text{H}$  NMR signals of the  $\text{CH}_2$  groups and the *ortho*-protons of the  $\text{C}_6\text{H}_4$ -*p*- $\text{NO}_2$  group shift 0.43 and 0.37 ppm (Fig. 2 (b)), respectively, to lower field relative to the corresponding signals of **2** (Fig. 2 (a)).

The results of further experiments incline us to assume that the other protonated form in Fig. 1 (b) is the species with the proton on a bridging thiolate. The addition of 4 equiv. of HOTf into the  $\text{CHCl}_3$  solution of **2** afforded an orange paste, which was quickly washed with  $\text{O}_2$ -free  $\text{CHCl}_3$  and dried *in vacuo*. The high-resolution mass spectrum ( $m/z$  604.9496) indicates that the orange paste is mainly composed of mono-protonated species of **2**. The orange paste displays two strong bands at the relatively high wavenumbers of 2112 and 2075  $\text{cm}^{-1}$  in the IR spectrum (Fig. 1, left (d)) and a signal at  $\delta = -1.09$  in its  $^{31}\text{P}\{^1\text{H}\}$  NMR spectrum (Fig. 1, right (d)) with a small signal from the  $\mu$ -hydride  $[\mathbf{2}(\text{FeHFe})]^+$  at  $\delta = 22.52$ . In the  $^1\text{H}$  NMR spectrum of the orange paste the signal of the  $\text{CH}_2$  groups of **2** at  $\delta = 4.20$  (Fig. 2 (a)) splits into two signals with marked down-field shifts to  $\delta = 6.66$  and 5.39 (Fig. 2 (c)), and the signals of aromatic protons of the  $\text{C}_6\text{H}_4$ -*p*- $\text{NO}_2$  group at  $\delta = 8.14$  and 6.68 for **2** also move to down field by 0.17 and 0.93 ppm, respectively. According to the spectroscopic evidence the P- and the bridging-N-protonated species can be ruled out for the orange paste, which is proposed to be the complex with one of the  $\mu$ -S atoms protonated,  $[\mathbf{2}(\text{SH})]^+$ . The additional signal at  $\delta = 3.05$  in the  $^1\text{H}$  NMR spectrum of the orange paste is tentatively assigned to the proton on the  $\mu$ -S atom.

Both  $^{31}\text{P}\{^1\text{H}\}$  and  $^1\text{H}$  NMR spectra suggest that  $[\mathbf{2}(\text{SH})]^+$  is the dominant component in the orange paste, which is contaminated with a small amount of  $[\mathbf{2}(\text{FeHFe})]^+$ . The protonation of one of the  $\mu$ -S atoms leads to a decrease in the electron-donating capability of the S atom, resulting in the decrease of the electron density of the iron atoms. Consequently the abated feedback bonds cause the great blue-shifts of  $\nu(\text{CO})$  frequencies of  $[\mathbf{2}(\text{SH})]^+$ . The splitting and the very large down-field shifts of the signals of the  $\text{CH}_2$  groups can be rationally explained by the proposed  $\mu$ -S-protonated species, which is suggested by theoretical calculations on the reaction mechanism at the diiron subsite of Fe-only hydrogenases but has not yet been identified by experiment.<sup>3</sup> Although the attempt to obtain a single crystal of  $[\mathbf{2}(\text{SH})]^+$  for an X-ray diffraction measurement was thwarted by the instability of  $[\mathbf{2}(\text{SH})]^+$  in solution, the structurally characterized  $[(\mu\text{-SCH}_2\text{CH}_2\text{SEt})\{\text{Fe}(\text{CO})_2(\text{PMe}_3)_2\}_2]^+[\text{OTf}]^-$ , obtained from the  $\mu$ -S-alkylation of  $[(\mu\text{-SCH}_2\text{CH}_2\text{S})\{\text{Fe}(\text{CO})_2(\text{PMe}_3)_2\}_2]$  with EtOTf in  $\text{CH}_2\text{Cl}_2$ ,<sup>13</sup> gives an indirect support for the argument of the  $\mu$ -S protonation of **2** in the presence of 4 equiv. of HOTf.

The molecular structures of **2** and its  $\mu$ -hydride diiron complex  $[\mathbf{2}(\text{FeHFe})]^+[\text{PF}_6]^-$  were determined by X-ray analyses of single crystals (Fig. 3).<sup>‡</sup> The  $\text{PMe}_3$ -disubstituted complex **2** exists in the crystalline state as two configurational isomers (Fig. 3 (top)), transoid basal-basal (ba-ba) and apical-basal (ap-ba). The two isomers pair up in a crystal cell. In contrast, the  $\text{PF}_6^-$  salt of

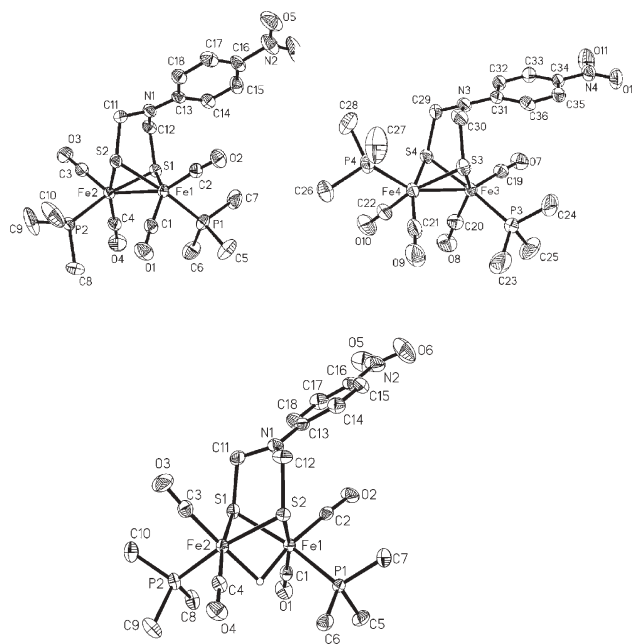


**Fig. 3** Molecular structures of two isomers of **2** (top) and the structure of  $[\mathbf{2}(\text{FeHFe})]^+$  (bottom) with thermal ellipsoids set at 30% probability. Selected distances ( $\text{\AA}$ ) and angles ( $^\circ$ ) for the ba-ba isomer of **2** (top, left): Fe1-Fe2 2.5671(10), Fe-P(av.) 2.2275(6), Fe-C<sub>CO</sub>(av.) 1.761(9), Fe-S(av.) 2.264(1), Fe1-S1-Fe2 69.15(4), S1-Fe1-S2 85.32(5), sum of angles at N1 357.7(9); for the ap-ba isomer of **2** (top, right): Fe3-Fe4 2.5280(14), Fe-P(av.) 2.223(1), Fe-C<sub>CO</sub>(av.) 1.763(5), Fe-S(av.) 2.275(6), Fe3-S3-Fe4 67.66(5), S3-Fe3-S4 85.04(5), sum of angles at N3 358.2(1); for  $[\mathbf{2}(\text{FeHFe})]^+$ : Fe1...Fe2 2.5879(8), Fe-H(av.) 1.75, Fe-P(av.) 2.2489(6), Fe-C<sub>CO</sub>(av.) 1.789(7), Fe-S(av.) 2.2713(4), Fe1-Fe2-H 41.5(16), Fe2-Fe1-H 42.9(15), Fe1-S1-Fe2 69.38(4), S1-Fe1-S2 84.46(4), sum of angles at N1 360.0(2).

$[\mathbf{2}(\text{FeHFe})]^+$  possesses the sole transoid ba–ba geometry (Fig. 3 (bottom)), which is identical with the coordination orientation of other reported  $\mu$ -hydride diiron analogues.<sup>4,8,9</sup> The crystallographic evidence indicates that a rotation of the  $\text{Fe}(\text{CO})_2\text{PMe}_3$  unit in the ap–ba isomer of **2** occurs during the protonation process of the iron atoms. In solution, the coordination configuration of **2** might be mobile structural forms.<sup>1a,5</sup> This kind of ligand-rotation phenomenon has been observed in the protonation processes of diiron and diruthenium propanedithiolates.<sup>4,8,14</sup> The general characteristics of the molecular structures, e.g. the butterfly framework of the  $2\text{Fe}_2\text{S}$  center, the pseudo-pyramidal coordination geometry of each iron atom in **2** and the distorted octahedral coordination sphere of the iron atoms in  $[\mathbf{2}(\text{FeHFe})]^+$ , are in agreement with previously reported  $2\text{Fe}_2\text{S}$  models.<sup>4,8,9</sup> The Fe–Fe bond in the ap–ba isomer of **2** is ca. 0.039 Å shorter than that in its ba–ba counterpart because of the smaller steric hindrance in the ap–ba orientation of the  $\text{PMe}_3$  ligands. The Fe–C<sub>CO</sub> and Fe–P coordination bonds are statistically indistinguishable in the two configurational isomers of **2**, while the mean Fe–S bond in the ap–ba isomer is 0.011(5) Å longer than that in the ba–ba geometry. The Fe···Fe distance (2.5879(8) Å) of  $[\mathbf{2}(\text{FeHFe})]^+$  shows a slight increase as compared to the corresponding ba–ba isomer (2.5671(10) Å) of **2**, in which there is an Fe–Fe bond. The mean Fe–C<sub>CO</sub> and Fe–P coordination bonds of the  $\mu$ -hydride complex are also lengthened by 0.027(8) and 0.021(4) Å, respectively, relative to the ba–ba isomer of **2**.

In this work, two protonated species of the diiron azadithiolate **2** were obtained and characterized. One is a  $\mu$ -hydride diiron complex  $[\mathbf{2}(\text{FeHFe})]^+$  and the other is assumed to be a  $\mu$ -S-protonated cation  $[\mathbf{2}(\text{SH})]^+$ , which is readily deprotonated in the presence of pyridine. The S atom is preferred over the N atom in the protonation process of **2** due to the weak basicity of the bridging-N, resulting from the strong electron-withdrawing  $\text{NO}_2$  group on the *para* position of the *N,N*-dialkylaniline. The results of this work provide indirect experimental evidence for the protonation capability of the  $\mu$ -S atoms in the diiron subsite of Fe-only hydrogenases. Further studies on protonation of diiron azadithiolate model complexes are under way.

We are grateful to the Natural Science Foundation of China (Grants 20471013 and 20128005), the Swedish Energy Agency and the Swedish Research Council for financial support of this work.

## Notes and references

† Crystal data for **2**:  $\text{C}_{18}\text{H}_{26}\text{Fe}_2\text{N}_2\text{O}_6\text{P}_3\text{S}_2$ ,  $M = 604.17$ ; monoclinic;  $P\bar{1}$ ;  $a = 13.248(3)$ ,  $b = 14.676(3)$ ,  $c = 15.028(3)$  Å,  $\alpha = 64.96(3)$ ,  $\beta = 82.40(3)$ ,

$\gamma = 82.83(3)^\circ$ ,  $V = 2616.4(9)$  Å<sup>3</sup>;  $\rho_{\text{calcd}} = 1.534$ ;  $\mu = 1.425$  mm<sup>-1</sup>;  $T = 293(2)$  K;  $Z = 4$ ;  $R_1 = 0.0485$  and  $wR_2 = 0.1174$  for 11823 reflections with  $I > 2\sigma(I)$ . CCDC 246474. Crystal data for  $[\mathbf{2}(\text{FeHFe})]^+[\text{PF}_6]^-$ :  $\text{C}_{18}\text{H}_{27}\text{F}_6\text{Fe}_2\text{N}_2\text{O}_6\text{P}_3\text{S}_2$ ,  $M = 750.15$ ; monoclinic;  $P2(1)/n$ ;  $a = 11.3070(6)$ ,  $b = 14.1755(5)$ ,  $c = 18.9123(9)$  Å,  $\alpha = 90.00$ ,  $\beta = 104.846(3)$ ,  $\gamma = 90.00^\circ$ ,  $V = 2930.1(2)$  Å<sup>3</sup>;  $\rho_{\text{calcd}} = 1.700$ ;  $\mu = 1.371$  mm<sup>-1</sup>;  $T = 293(2)$  K;  $Z = 4$ ;  $R_1 = 0.0531$  and  $wR_2 = 0.1382$  for 7212 reflections with  $I > 2\sigma(I)$ . CCDC 279852. For crystallographic data in CIF or other electronic format see DOI: 10.1039/b513270c

- (a) I. P. Georgakaki, L. M. Thomson, E. J. Lyon, M. B. Hall and M. Y. Darensbourg, *Coord. Chem. Rev.*, 2003, **238–239**, 255–266; (b) D. J. Evans and C. J. Pickett, *Chem. Soc. Rev.*, 2003, **32**, 268–275; (c) T. B. Rauchfuss, *Inorg. Chem.*, 2004, **43**, 14–26; (d) L. Sun, B. Åkermark and S. Ott, *Coord. Chem. Rev.*, 2005, **249**, 1653–1663.
- (a) Z. Cao and M. B. Hall, *J. Am. Chem. Soc.*, 2001, **123**, 3734–3742; (b) H. Fan and M. B. Hall, *J. Am. Chem. Soc.*, 2001, **123**, 3828–3829.
- (a) M. Bruschi, P. Fantucci and L. D. Gioia, *Inorg. Chem.*, 2002, **41**, 1421–1429; (b) T. Zhou, Y. Mo, A. Liu, Z. Zhou and K. R. Tsai, *Inorg. Chem.*, 2004, **43**, 923–930.
- X. Zhao, I. P. Georgakaki, M. L. Miller, R. Mejia-Rodriguez, C. Chiang and M. Y. Darensbourg, *Inorg. Chem.*, 2002, **41**, 3917–3928.
- J. L. Nehring and D. M. Heinekey, *Inorg. Chem.*, 2003, **42**, 4288–4292.
- R. Mejia-Rodriguez, D. Chong, J. H. Reibenspies, M. P. Soriaga and M. Y. Darensbourg, *J. Am. Chem. Soc.*, 2004, **126**, 12004–12014.
- (a) J. Capon, S. E. Hassnaoui, F. Gloaguen, P. Schollhammer and J. Talarmin, *Organometallics*, 2005, **24**, 2020–2022; (b) J. W. Tye, J. Lee, H.-W. Wang, R. Mejia-Rodriguez, M. B. Hall and M. Y. Darensbourg, *Inorg. Chem.*, 2005, **44**, 5550–5552.
- F. Gloaguen, J. D. Lawrence, T. B. Rauchfuss, M. Bénard and M. Rohmer, *Inorg. Chem.*, 2002, **41**, 6573–6582.
- X. Zhao, I. P. Georgakaki, M. L. Miller, J. C. Yarbrough and M. Y. Darensbourg, *J. Am. Chem. Soc.*, 2001, **123**, 9710–9711.
- (a) M. Schmidt, S. M. Contakes and T. B. Rauchfuss, *J. Am. Chem. Soc.*, 1999, **121**, 9736–9737; (b) F. Gloaguen, J. D. Lawrence and T. B. Rauchfuss, *J. Am. Chem. Soc.*, 2001, **123**, 9476–9477; (c) D. Chong, I. P. Georgakaki, R. Mejia-Rodriguez, J. Sanabria-Chinchilla, M. P. Soriaga and M. Y. Darensbourg, *Dalton Trans.*, 2003, 4150–4163.
- (a) J. D. Lawrence, H. Li, T. B. Rauchfuss, M. Bénard and M. Rohmer, *Angew. Chem.*, 2001, **113**, 1818–1821, *Angew. Chem., Int. Ed.*, 2001, **40**, 1768–1771; (b) S. Ott, M. Kritikos, B. Åkermark, L. Sun and R. Lomoth, *Angew. Chem.*, 2004, **116**, 1024–1027, *Angew. Chem. Int. Ed.*, 2004, **43**, 1006–1009; (c) T. Liu, M. Wang, Z. Shi, H. Cui, W. Dong, J. Chen, B. Åkermark and L. Sun, *Chem.–Eur. J.*, 2004, **10**, 4474–4479; (d) F. Wang, M. Wang, X. Liu, K. Jin, W. Dong, G. Li, B. Åkermark and L. Sun, *Chem. Commun.*, 2005, 3221–3223; (e) P. Das, J. Capon, F. Gloaguen, F. Y. Pétillon, P. Schollhammer and J. Talarmin, *Inorg. Chem.*, 2004, **43**, 8203–8205.
- J. D. Lawrence, H. Li and T. B. Rauchfuss, *Chem. Commun.*, 2001, 1482–1483.
- X. Zhao, C. Chiang, M. L. Miller, M. V. Rampersad and M. Y. Darensbourg, *J. Am. Chem. Soc.*, 2003, **125**, 518–524.
- A. K. Justice, R. C. Linck, T. B. Rauchfuss and S. R. Wilson, *J. Am. Chem. Soc.*, 2004, **126**, 13214–13215.